Composites: Part A 90 (2016) 451–456

Contents lists available at ScienceDirect

Composites: Part A

journal homepage: www.elsevier.com/locate/compositesa

# Understanding the buckling behaviour of steered tows in Automated Dry Fibre Placement (ADFP)

M.Y. Matveev *, P.J. Schubel, A.C. Long, I.A. Jones

*Composites Group, Faculty of Engineering, The University of Nottingham, UK*

ARTICLE INFO

*Article history:*
Received 11 June 2016
Received in revised form 9 August 2016
Accepted 13 August 2016
Available online 16 August 2016

*Keywords:*
B. Defects
C. Analytical modelling
C. Process modelling
E. Automated Fibre Placement (AFP)

ABSTRACT

Technologies for automated fibre lay-up have proven their usefulness in composites manufacturing. Further development of the technologies, such as Automated Dry Fibre Placement (ADFP), allow further reduction of waste and increase of the design space through tow steering which enables creation of composites with tailored properties. Tow steering is, however, limited by possible defects such as wrinkles which result from mismatch of fibre length and steering path. This paper addresses wrinkle formation at different steering radii and provides a closed-form solution for the problem. Experimental results are used for estimation of the model parameters and validation of the model. An analytical framework is used to explore effects of processing parameters on defect formation. It was found that the tack stiffness has the greatest influence on defect formation. Parametric studies showed that increase of the temperature within the admissible temperature window can improve the tack properties and hence improve the lay-up.



## 1. Introduction

Automated lay-up technologies provide an opportunity to reduce manufacturing costs by reducing waste of material during fibre preforming and potentially increase production rate. Two main variants of automated lay-up are Automated Tape Lay-up (ATL) which operates with wide tapes (~100 mm width) and Automated Fibre Placement (AFP) which operates with up to 32 tapes (usually called tows) each with typical width between 3 mm and 12 mm [1]. In both cases, the lay-up is aided by a head which feeds and compacts the tapes in a single automated operation. One of the main advantages of AFP technology over ATL is its ability to cut each of the narrow tapes separately, hence further reducing waste. Prepreg tapes are the current standard material used in ATL/AFP, however there are current developments in using dry fibre tapes. The "dry tows" are typically non-impregnated slit unidirectional carbon fibre coated with a thermoplastic binder on one side and a mesh substrate (thermoplastic or glass fibre veil) on the other side. AFP makes it possible to utilise in full the concept of variable-angle tow composites by steering tows during lay-up [2,3]. This vastly expands the design space and allows the design of components which have improved stiffness, buckling or other properties when compared to non-steered laminates [4]. However, steering of the tapes can be challenging due to limitations on path curvature, lay-up speed and other parameters. The main challenge of automated lay-up is to achieve the control of defects such as out-of-plane wrinkles and tow pull ups. Both of these are the result of mismatching tow length and steering path and hence excessive compression or tensile force which buckles or lifts tows beyond the point they can be held by adhesive forces. It has been reported that it is possible to achieve defect-free lay-up with a minimum steering radius of 0.5 m for some material systems [1]. One of the possible alternatives to tow steering is adoption of continuous tow sheering which is less susceptible to wrinkling [5]. However, it still remains unclear how the minimum steering radius can be predicted prior the manufacturing and, more importantly, whether steering radius can be linked directly to the occurrence of defects in the lay-up.

There is strong dependence between the tackiness of the tows (either "dry" or prepreg) and how well the tow conforms to a substrate [1,6,7]. At the same time, the tackiness depends on the process parameters such as temperature, pressure and time [6,7]. Analysis of prepreg conformance to a substrate was carried out by Gutowski and Bonhomme [8] for a problem of end curling in prepregs using Newtonian squeeze flow theory in combination with beam bending analysis. The analysis provided bounds for lay-up speed and consolidation force for given prepreg parameters but did not include the effects of temperature. Several works were devoted to estimation of interlaminar or bonding strength

* Corresponding author.
*E-mail address:* Mikhail.Matveev@nottingham.ac.uk (M.Y. Matveev).

http://dx.doi.org/10.1016/j.compositesa.2016.08.014
1359-835X/

of AFP-made laminates using the concept of "healing" or diffusion of polymer across contacting surfaces [5,6]. This approach demonstrated the ability to predict the trends in evolution of these parameters with change of process parameters which can be used for optimisation of the manufacturing process and evaluation of the properties of the interface between the tow and the substrate [9–11]. Wrinkling (or buckling) during in-plane tow steering was explored by Beakou et al. [12] who employed elastic buckling analysis to describe the problem. Interface between the dry tow and substrate was represented as an elastic foundation which allowed linking of the tackiness and the minimum steering radius. However, this approach was based on a constant size parameter, the value of which was not justified.

This paper focuses on the theoretical analysis for the lay-up of a steered dry tows using an ADFP facility. Limited experimental results are presented in Section 2 and used for estimation of the model parameters. Section 3 outlines the main assumptions and considerations for mechanical modelling of steering for dry tows. The main concept of the mechanical analysis is to consider wrinkling as elastic buckling of a plate and hence individual manifestations of buckling will be referred to as wrinkles in this publication. The tow is treated as an orthotropic solid plate on elastic foundation under non-uniform compressive load with appropriate boundary conditions developed from the approach by Beakou et al. [12] and with a clear link to physical parameters. The resulting closed-form solution for buckling load is analysed in terms of steering radius and stiffness of elastic foundation. The previously mentioned polymer "healing" theory is applied in Section 4 for a parametric analysis of process parameters on the quality of lay-up. Section 5 discusses applicability and limitations of the modelling approach and implications of the parametric study in Section 4 on the practical aspects of the tow steering. Section 6 gives overall conclusions and recommendations for practical use of AFP machines.

## 2. Experiments

A Coriolis AFP machine with an eight tow feed head and 6.35 mm width individual tows was used to perform several dry tow steering trials. The material was unidirectional carbon fibre 24 K slit tapes with areal weight of 194 gsm coated with a thermoplastic binder on one side and a glass fibre veil on the other side. The purpose of the trials was qualitative assessment of behaviour of tows when laid down at various steering radii. The tows were laid on a three layer [90°/0°/90°] substrate made of the same material. The radii were 1.5, 1.2, 0.9, 0.7, 0.5 and 0.4 m. The roller pressure was controlled at 200 N with a deposition speed set at 1 m/s. Tow deposition temperature was controlled by a laser heating system mounted on the AFP head. The laser heating system is power controlled with no thermal feedback, and was set at 800 W for this study. A thermal camera was fitted to monitor the temperature during the lay-up, which registered typical temperatures of 250 °C at the outer surface of the tows. Several examples of the lay-up are shown in Fig. 1. It can be seen that wrinkling due to buckling occurs in all the steering paths at the inner radii which indicates that tows are too stiff and tack is too low to accommodate the imposed compressive deformations. It can also be noted that the wrinkling is relatively regular along a tow length and it can be considered to be periodic in the first approximation. The main difference between the tows laid at different steering radii is the frequency of wrinkles and their length. The wavelength of wrinkles was measured manually by counting the number of wrinkles per 1 m of tow length and is given in Table 1. The wavelength of wrinkles was measured for an inner tow only but it is expected that the wavelengths for adjacent tows are relatively close to each other.

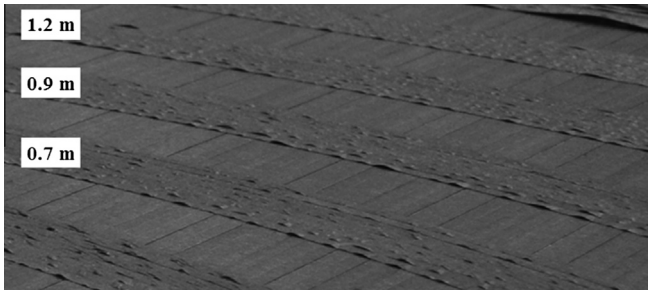


**Fig. 1.** Example of wrinkles in steered tows at radii of 1.2, 0.9, 0.7 m (from top to bottom).

**Table 1**
Wavelength of wrinkles.

| Radius, m | 2.0[a] | 1.5 | 1.2 | 0.9 | 0.7 | 0.5 | 0.4 |
|---|---|---|---|---|---|---|---|
| Wavelength, cm | 4.21 | 1.95 | 1.56 | 1.35 | 1.19 | 1.07 | 1.02 |

[a] Lay-up at 650 W laser power.

## 3. Modelling of tow steering

The main reason for out-of-plane wrinkling of tows is mismatch of the imposed geometrical path and the tow length. If a tow is laid on a curved path then it will result in combined compressive and tensile load applied through the width of the tow, with the exact distribution depending on how the steering path is imposed. In principle, the applied compressive load leads to the top buckling and tensile load leads to tape pull up. This paper considers only tow buckling due to dominant compressive forces.

Observation of the produced sample for the steered tows (Fig. 1) shows that multiple wrinkles form within an individual tow and that the wrinkles are spaced approximately uniformly along the length of the tow. However, it is noteworthy that, since the tow lay-up is a continuous process, wrinkles are more likely to form one by one during the process. As the lay-up progresses and the length of tow laid increases, at some point the tow buckles and releases excessive load. This buckling occurs in the first buckling mode which usually corresponds to the lowest load for short beams and plates. However, buckling is opposed by tack between the tow and substrate and this increases the critical buckling load. This also means that the postbuckling shape of the tow in the presence of tack will result in both delaminated and intact parts of the interface i.e. a wrinkle will localise in the centre leaving the rest of the tape having no deflection. Once the tow has buckled and wrinkled locally, the process continues until the newly deposited tow is long enough to buckle again. Therefore, it is proposed to consider each wrinkle in isolation from previous wrinkles.

### 3.1. Buckling of an orthotropic plate under non-uniform load

The wrinkling problem can be considered to be equivalent to the buckling of an annular orthotropic homogenous solid plate on an elastic foundation. However, since curvature of the tow and its length (spacing between wrinkles) are relatively small it is more practical to consider the problem as the buckling of a rectangular orthotropic plate. Only buckling at the inner edge is investigated in this problem and hence the plate is free at its inner edge, simply supported at its outer edge and clamped at its radial edges. Clamped radial edges represent good conformance of the tow and substrate between the wrinkles. These boundary conditions are

quite different from those proposed by Beakou et al. [12] and are thought to be more realistic. A diagram of the problem is shown in Fig. 2.

The load applied to the plate originates from mismatch of tape length and the paths for the inner and outer radius imposed on the tape by steering. Both of the paths are defined by its radius only and it can be assumed that there is a "neutral" radius, $R$, at which there is no length mismatch along the tape length. The mismatch of the lengths results in a compressive load, $P$, defined as:

$$P(y) = P_0\left(1 - \frac{\alpha y}{b}\right) \tag{1}$$

where $b$ is the width of the plate equal to the width of dry tow, $P_0$ is load applied at the inner edge of the plate. The load $P_0$ is related to the steering radius in Section 3.3. Coefficient $\alpha$ defines the non-uniformity of the load. The case of $\alpha = 0$ corresponds to uniform compression, $\alpha = 1$ corresponds to compression load decaying from the inner edge to the outer edge and $\alpha = 2$ corresponds to pure bending i.e. equal tension and compression.

The differential equation describing the bending of an isotropic plate on an elastic foundation is given as:

$$\nabla^2 w + kw = P \tag{2}$$

where $w$ is plate deflection and $k$ is stiffness of elastic foundation.

The kinematic boundary conditions for this problem are:

$$\begin{aligned} &w(x=0) = 0 \\ &w'(x=0) = 0 \\ &w(x=L) = 0 \\ &w'(x=L) = 0 \\ &w(y=b) = 0 \end{aligned} \tag{3}$$

The edge at $y = 0$ is free of forces and torques, and there is also no torque at $y = b$.

This problem has an exact solution in hyperbolic functions (and in Bessel functions for the analogous annular plate problem) which becomes complex for an orthotropic plate with given boundary conditions (mainly due to free edge conditions) as noted by Timoshenko and Grigolyuk [13]. An approximate solution can be derived using the approach outlined by Timoshenko for a similar

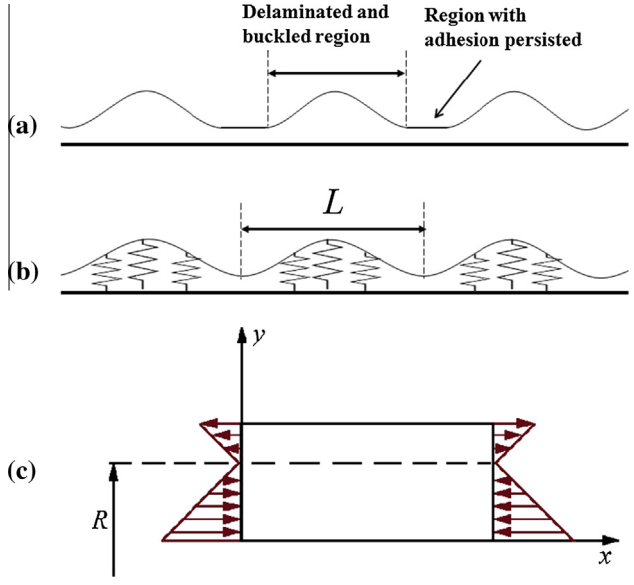


**Fig. 2.** Diagram of the buckling problem: (a) tow wrinkling with partial delamination; (b) model of plate on elastic foundation; (c) section of a plate under non-uniform load. (For interpretation of the references to colour in this figure legend, the reader is referred to the web version of this article.)

case [13]. According to the Rayleigh-Ritz approach, the assumed solution should fulfil only kinematic boundary conditions (3). The Rayleigh-Ritz approach was used for a related problem of buckling of variable angle tow plates earlier e.g. by Wu et al. [14].

The Rayleigh-Ritz approach dictates that the total energy, $\Pi$, should be minimised with respect to its amplitude:

$$\frac{\partial \Pi}{\partial c_i} = 0 \tag{4}$$

where $\Pi$ is total energy of the system equal to combination of elastic strain energy, $U$, energy stored in the elastic foundation, $K$, and work by applied load, $Q$:

$$\Pi = U + K - Q \tag{5}$$

Elastic strain energy, energy of foundation and work made by applied load are found as:

$$U = \frac{1}{2}\int_0^L \int_0^b \left( D_{11}\left(\frac{\partial^2 w}{\partial x^2}\right)^2 + D_{22}\left(\frac{\partial^2 w}{\partial y^2}\right)^2 + 2D_{12}\frac{\partial^2 w}{\partial x^2}\frac{\partial^2 w}{\partial y^2} + 4D_{66}\left(\frac{\partial^2 w}{\partial x \partial y}\right)^2 \right) dxdy \tag{6}$$

$$K = \frac{1}{2}\int_0^L \int_0^b kw^2 dxdy \tag{7}$$

$$Q = \frac{1}{2}P_0 \int_0^L \int_0^b \left(1 - \frac{\alpha y}{b}\right)\left(\frac{\partial w}{\partial x}\right)^2 dxdy \tag{8}$$

The form of an approximate solution can be chosen to be close to a function defining the applied load (1) and be convenient for closed-form solution as e.g. in [15]. The solution can be assumed to be given by:

$$w(x,y) = \sum_{i=1}^{n} c_i \left(1 - \frac{y}{b}\right)^{i+1}\left(1 - \cos\left(\frac{2\pi m x}{L}\right)\right) \tag{9}$$

where $b$ and $L$ are width and length of the tow section, $m$ is the number of waves in a buckling mode and $c_i$ are amplitude coefficients. While it was discussed earlier that only the first buckling mode is of interest in this problem, the solution will be generalised for higher buckling modes.

Substitution of function (9) into Eqs. (6)–(8) can be generalised for any number of terms but this is impractical. By using only one term of the displacement function (9), the critical load is found to be (exact derivation of energies is given in Appendix A):

$$P_{cr} = \frac{1}{6 - \alpha}\left(24D_{11}\left(\frac{\pi m}{L}\right)^2 + 160D_{66}\left(\frac{1}{b}\right)^2 - 40D_{12}\left(\frac{1}{b}\right)^2 + 90D_{22}\left(\frac{L}{\pi m b^2}\right)^2 + \frac{9}{2}k\left(\frac{L}{\pi m}\right)^2\right) \tag{10}$$

The results can be refined by using more terms in the deflection function. The difference between the solutions obtained using one term (Eq. (10)) and two or three terms in representation of displacement, $w$, (Eq. (9)) are 3.9% and 4.1% respectively for $\alpha = 1$. The difference increases with increase of parameter $\alpha$ and the corresponding values are 15% and 16% for $\alpha = 2$.

Parameter $\alpha$, which governs non-uniformity of the load, has a strong effect on the solution. The special case is $\alpha = 6$ when the solution becomes singular i.e. the buckling load is infinite. However, it should be pointed out that for the loading case when $\alpha > 2$ i.e. the tensile load prevails over the compressive load, buckling is expected at the outer edge and the problem should be adapted by assuming that the inner edge is simply supported.

### 3.2. Estimation of parameters

Eq. (10) for the critical buckling load includes material parameters of the tow and the stiffness of the elastic foundation. The bending rigidity of the tow was measured by a simple overhang test using a 15 cm long tow clamped horizontally at one end and a small mass at the other end. The tow was assumed to deform as an Euler-Bernoulli beam and its total deflection at the end was used to extract its Young's modulus, $E_1$, which was found to be equal to 30 GPa. The difference between this value and the anticipated tensile Young's modulus of carbon fibre tow probably arises from inter-tow slippage of fibre and from the non-homogeneity of the tow. The bending stiffness of the plate was calculated as:

$$D_{11} = \frac{E_1 h^3}{12(1 - v_{12}v_{21})} \tag{11}$$

where $h$ is the tow thickness and $v_{12} = 0.2$, $v_{21} = 0.02$ are the assumed Poisson's ratios of the tow.

There are no means to characterise other stiffness parameters of the tape, $D_{22}, D_{12}$ and $D_{66}$. However, since all the fibres are aligned in one direction only and the tow is dry, it can be assumed that the tape is highly anisotropic i.e. $D_{22}, D_{12}$ and $D_{66}$ are orders of magnitude smaller than $D_{11}$. A brief sensitivity study shows that the predicted critical buckling load with an assumed ratio between stiffness of 100 times is within 2% of the load if the ratio is assumed to be 50 times. This shows insignificance of exact values of these parameters and hence a factor of 100 will be used for $D_{22}, D_{12}$ and $D_{66}$ within the calculations below.

The stiffness of the elastic foundation is also an unknown parameter as it has never been measured for the given system. The parameter $k$ will be estimated using experimental data in Section 3.3.

### 3.3. Critical steering radius

Eq. (10) gives the critical buckling load for a plate under non-uniform load but does not link it to parameters of the steering path. Moreover, in the steering problem the load remains constant while the length of the tape increases. This constant load from steering, which originates from the mismatch of the tow length and path length. This mismatch can be derived by assuming that the tow was steered at radius $R$ over an arbitrary angle $\theta$ so that is has a length $\theta R$. It should be noted that the radius $R$ corresponds to some "neutral" line, at which there is no length mismatch. The other parts of the tow have a length mismatch which depends on coefficient $\alpha$ (see Fig. 1). The internal edge of the tow has length of $\theta(R - b/\alpha)$ and hence the strain arising from the mismatch is equal to $b/(\alpha R)$. Consequently, the maximum amplitude of the distributed load (1) can be written as:

$$P_0 = \frac{E_1 h b}{\alpha R} \tag{12}$$

where $E_1$, $h$ and $R$ are respectively the Young's modulus of the tow, tow thickness and steering radius.

Therefore, the buckling problem should be treated slightly differently in application to the steering problem. In the case when the critical load given by Eq. (10) is higher than (12), then tow remains unbuckled. If the critical load given by Eq. (10) is lower than the load from steering (12), then the tow buckles and the wavelength of the wrinkle, $L$, should be found from solving these two equations. This leads to a simple biquadratic equation:

$$\left(90D_{22}\left(\frac{1}{\pi m b^2}\right)^2 + \frac{9k}{2(\pi m)^2}\right)L^4 + \left(\frac{160D_{66}}{b^2} - 40D_{12}\left(\frac{1}{b}\right)^2 + (6-\alpha)\frac{Ehb}{\alpha R}\right)L^2 + 24D_{11}(\pi m)^2 = 0 \tag{13}$$

Eq. (12) can be used to fit the unknown parameter $k$ using experimental data from Table 1. For radius $R$ = 1.5 m it was found that k = 2.25 × $10^8$ N/m$^3$ gives the closest value to the experimental wrinkle wavelength. Higher stiffness values yields no solution which corresponds to no defects (infinite wavelength). Model predictions of the wrinkling wavelength with this parameter and parameters from Table 2 are given in Fig. 3. It can be seen that the present approach is able to predict the trend of decreasing wrinkling wavelength with decrease of the steering radius.

The most useful case is when the critical load is equal to the load induced by steering, corresponding to the threshold between buckling and no buckling. This condition can be used to find the critical steering radius. First of all, Eq. (10) is differentiated with respect to $L$ and the minimum load is found. This load is then equated to the load given by (12) and the critical radius $R_{cr}$ can be found as:

$$R_{cr} = \frac{(6-\alpha)Ehb^3\sqrt{20D_{22} + b^4kD_{11}}}{4\alpha\left(3\sqrt{3}D_{11}b^4k - 10D_{12}\sqrt{20D_{22} + b^4kD_{11}} + 40D_{66}\sqrt{20D_{22} + b^4kD_{11}} + 60\sqrt{3}D_{22}D_{11}\right)} \approx \frac{(6-\alpha)Ehb^3}{4\alpha\left(3\sqrt{3D_{11}k}b^2 - 10D_{12} + 40D_{66} + 60\sqrt{3D_{11}/(b^4k)}D_{22}\right)} \tag{14}$$

where $D_{22} \ll b^4kD_{11}$ was assumed.

The critical radius as given by Eq. (14) is shown in Fig. 4 for a range of tow widths and values of stiffness parameter $k$. Obviously, a larger tow width requires a larger steering radius to produce no wrinkling. It can be deduced from Eq. (14) that the critical radius $R_{cr}$ is proportional to the tape width $b$ and $R_{cr} \propto 1/\sqrt{k}$ for larger values of $k$.

## 4. Effect of process parameters on the tack and steering radius

The effect of elastic foundation stiffness on the critical steering radius was explored in the previous section. Meanwhile, the stiffness of the elastic foundation, representing the tack, depends on the processing conditions such as temperature, deposition pressure and speed. Several works [9,11] successfully implemented

**Table 2**
Model parameters.

| b, mm | h, mm | E, GPa | k, N/m$^3$ | $D_{11}$, Nm |
|---|---|---|---|---|
| 6.35 | 0.25 | 30 | 2.25 × $10^8$ | 0.039 |

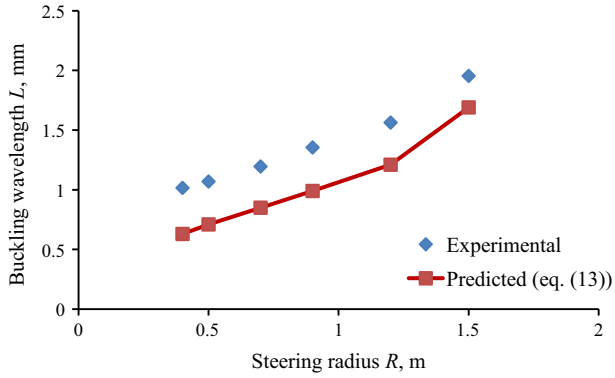


**Fig. 3.** Dependency of wrinkling wavelength on steering radius. (For interpretation of the references to colour in this figure legend, the reader is referred to the web version of this article.)

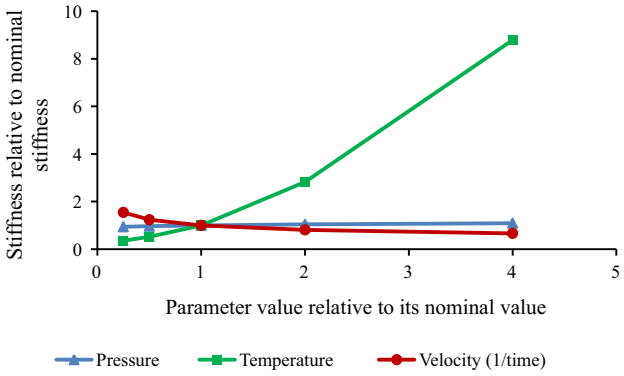


**Fig. 5.** Parametric studies in Eq. (15) using parameters from [9]. Parameters were varied one at a time by scaling the nominal values by factor of 0.25, 0.5, 2 and 4. (For interpretation of the references to colour in this figure legend, the reader is referred to the web version of this article.)

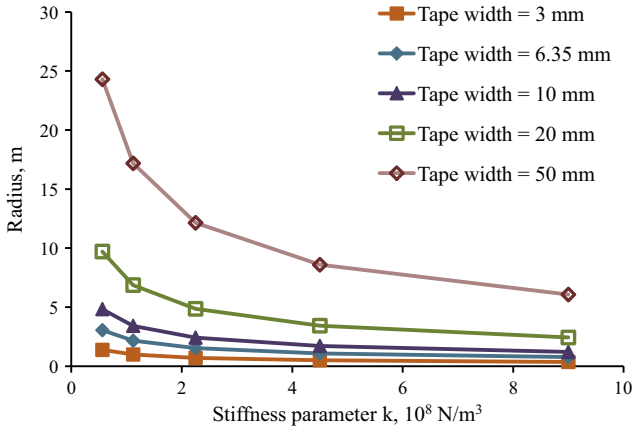


**Fig. 4.** Effect of tow width and stiffness parameter on critical steering radius. (For interpretation of the references to colour in this figure legend, the reader is referred to the web version of this article.)

healing and intimate contact theories to describe the interlaminar strength of an AFP lay-up in terms of the mentioned process parameters. One of the assumptions of the healing theory is that the strength increases with increase of the contact area between two surfaces. It can be also assumed that the stiffness of the elastic foundation, i.e. stiffness of bond between two surfaces is also proportional to the contact area. The aforementioned theories attempt to describe the process in terms of the characteristic time required for achieving perfect contact and perfect diffusion, so-called welding time. These characteristic times are then compared to the overall process time. By employing this approach, the dependence of the stiffness parameter in the buckling model on process parameters can be established.

According to the chosen approach, the degree of healing is the ratio of current interface properties to their maximum values. In the case of an isothermal process, the healing parameter, $D_h$, is defined as [9]:

$$D_h \propto \left(\frac{t}{t_w(T)}\right)^{1/4}\left(\frac{t}{t_w(T)}\right)^{1/4}\left(1+A\frac{Pt}{\mu(T)}\right)^{1/5} \tag{15}$$

where $A$ is a material parameter, $t$, $t_w$ and $\mu$ are process time, welding time and viscosity. The functions which describe the welding time and viscosity are an exponential function of inverse temperature being proportional to $\exp(-BT^{-1})$. Details regarding parameters $A$ and B can be found in [9].

Parameters required to calculate the degree of healing using Eq. (15) are non-trivial to measure and require separate characterisation for every material system. However, it is still possible to perform parametric analysis relying on some representative values and general analysis of the analytical function (15). It can be seen that increasing the processing time, $t$, and applied pressure, $P$, increases function (15). It has to be noted that processing time is implicitly defined by the lay-up speed, $v$, i.e. $t \propto 1/v$. In other words, a slower deposition speed with higher compaction force will result in stronger and stiffer interface between the tow and the substrate. However, the increase in absolute values is relatively small as shown in Fig. 5.

The degree of healing depends on temperature due to assumptions that the diffusion process progresses faster for materials with lower viscosity and higher mobility of polymer chains. This phenomenon is empirically described by inserting functions for viscosity and welding time into Eq. (15) in the form of an exponential function of temperature. These exponential terms have a significant effect on the degree of healing as shown in Fig. 5. The overall effect of processing parameters can be summarised as follows:

$$k \propto D_h \propto f(v^{-0.5}, P^{0.2}, \exp(T)) \tag{16}$$

## 5. Discussion

The mechanical model presented in this work is based on several assumptions. First of all, the tows used in ADFP are assumed to be homogeneous and to behave like a solid elastic orthotropic plate. While the assumptions are reasonable for relatively rigid dry tapes, the latter assumption might be not valid for prepreg tows which exhibit viscoelastic properties at high temperatures. Moreover, such prepreg tows might exhibit additional buckling modes which will accommodate excessive length in the in-plane waviness of fibres. However, this case of transverse buckling is out of scope for the presented modelling approach.

It was assumed that the buckling process completely ignores possible nonlinearities due to energy dissipation through delamination. One of the possible discrepancies arising from neglecting delamination is incorrect description of the post-buckling localisation of the wrinkle. This effect has already been studied [16–18] for the case of thin films on rigid substrate where a film buckles with high buckling mode due to compression or thermal stresses and then progressively delaminates with localisation of a wavy surface into one dominating wrinkle. This process is possible in systems which can sustain high buckling modes without any delamination but is very unlikely here due to low tack and energy release rate.

Furthermore, it is assumed that after buckling the tow immediately transforms into a fully delaminated state neglecting the progressive delamination and actual energy release rate. It is expected that the present approach results in prediction of the lower critical buckling load for a given plate length and underpredicting wrinkling wavelength.

The analytical approach presented in this work is able to predict the critical load which can be used to find the minimum tow steering radius, but can also predict wrinkling wavelength if the radius is below the minimum radius. This can be beneficial in predicting the quality of the layup i.e. the amplitude and the amount of the wrinkles in a given layup.

The analytical representation of the problem makes it possible to explore the effect of system parameters on the minimum steering radius. It was found that the minimum steering radius is proportional to the square root of inverse stiffness of the elastic foundation ($\propto 1/\sqrt{k}$). The analysis of the stiffness of elastic foundation in terms of the process parameters showed that processing temperature has the largest impact. It was found that increase of temperature results in exponential growth of the stiffness. Since the stiffness of the elastic foundation (tack stiffness) is one of the key parameters in the buckling model it is possible to draw several practical conclusions. One of the obvious results is that any tack improvement leads to improved quality of the lay-up. Next, higher deposition pressure and slower deposition rate both increase tack and hence improve the lay-up. However, effect of these two parameters on tack is relatively small when compared to the effect of temperature. This makes temperature a key parameter as an increase in the temperature should lead to better quality of the lay-up. This provides an opportunity to improve the quality of lay-up by adjusting the process parameters. However, it should be noted that temperature change should still remain in the admissible range to melt the polymer binder but not to degrade it.

## 6. Conclusion

The paper presents an analytical approach for prediction wrinkling of tows during ADFP. The approach ties together several process parameters: steering radius, deposition temperature, pressure and speed. The main components of the approach are in the solution of the buckling problem by approximate methods and the "healing" theory of polymers. The solution of the buckling problem was validated on limited experimental data and was found to be able to predict correct trends for wrinkling wavelength with change of steering radius. A closed-form solution for the critical steering radius was also derived.

A theory of polymer healing was used to assess the effects of process parameters on the wrinkling wavelength and critical steering radius. It was found that processing temperature has the strongest effect on the stiffness of elastic foundation and hence on formation of the defects. It was concluded that increase in the lay-up temperature leads to lower critical steering radius i.e. improves the lay-up quality.

## Acknowledgements

This work was supported by the Engineering and Physical Sciences Research Council [grant number: EP/K031430/1], through the "Robustness-performance optimisation for automated composites manufacture" project. The authors would like to express their gratitude to the National Composite Centre (NCC), Bristol, UK for help with experimental ADFP trials.

## Appendix A

The solution in form of (9) was substituted in Eqs. (6)–(8) and elastic strain energy, energy of foundation and work done by applied load are as follows:

$$U = c_1^2\left(\frac{4}{5}D_{11}bL\left(\frac{\pi m}{L}\right)^4 + \frac{(16D_{66}-4D_{12})}{3}\frac{b}{L}\left(\frac{\pi m}{L}\right)^2 + \frac{3D_{22}L}{b^3}\right) \quad (A.1)$$

$$K = c_1^2\frac{3kbL}{20} \quad (A.2)$$

$$Q = c_1^2(6-\alpha)\left(\frac{\pi m}{L}\right)^2\frac{bL}{30}P \quad (A.3)$$

These expressions are then substituted into Eq. (4) and differentiated with respect of $c_1$ and resolved with respect of $P$ resulting in Eq. (10).

## References

[1] Lukaszewicz DHJA, Ward C, Potter KD. The engineering aspects of automated prepreg layup: history, present and future. Compos Part B – Eng 2012;43(3):997–1009.
[2] Gurdal Z, Olmedo R. Inplane response of laminates with spatially varying fiber orientations – variable stiffness concept. AIAA J 1993;31(4):751–8.
[3] Paul W, Kevin P, Kalyan H, Marvin S, Mattew H. Buckling of variable angle tow plates: from concept to experiment. In: 50th AIAA/ASME/ASCE/AHS/ASC structures, structural dynamics, and materials conference. American Institute of Aeronautics and Astronautics; 2009.
[4] Gurdal Z, Tatting BF, Wu CK. Variable stiffness composite panels: effects of stiffness variation on the in-plane and buckling response. Compos Pt A – Appl Sci Manuf 2008;39(5):911–22.
[5] Kim BC, Potter K, Weaver PM. Continuous tow shearing for manufacturing variable angle tow composites. Compos Pt A – Appl Sci Manuf 2012;43(8):1347–56.
[6] Crossley RJ, Schubel PJ, De Focatiis DSA. Time-temperature equivalence in the tack and dynamic stiffness of polymer prepreg and its application to automated composites manufacturing. Compos Pt A – Appl Sci Manuf 2013;52:126–33.
[7] Crossley RJ, Schubel PJ, Warrior NA. The experimental determination of prepreg tack and dynamic stiffness. Compos Pt A – Appl Sci Manuf 2012;43(3):423–34.
[8] Gutowski TG, Bonhomme L. The mechanics of prepreg conformance. J Compos Mater 1988;22(3):204–23.
[9] Grouve WJB, Warnet LL, Rietman B, Visser HA, Akkerman R. Optimization of the tape placement process parameters for carbon-PPS composites. Compos Pt A – Appl Sci Manuf 2013;50:44–53.
[10] Heider D, Piovoso MJ, Gillespie JW. A neural network model-based open-loop optimization for the automated thermoplastic composite tow-placement system. Compos Pt A – Appl Sci Manuf 2003;34(8):791–9.
[11] Khan MA, Mitschang P, Schledjewski R. Parametric study on processing parameters and resulting part quality through thermoplastic tape placement process. J Compos Mater 2013;47(4):485–99.
[12] Beakou A, Cano M, Le Cam JB, Verney V. Modelling slit tape buckling during automated prepreg manufacturing: a local approach. Compos Struct 2011;93(10):2628–35.
[13] Timoshenko SP, Grigolyuk EI. Stability of bars, plates and shells. Collection of works. Nauka; 1971.
[14] Wu ZM, Weaver PM, Raju G, Kim BC. Buckling analysis and optimisation of variable angle tow composite plates. Thin-Walled Struct 2012;60:163–72.
[15] Paul W, Herencia J. Buckling of a flexurally anisotropic plate with one edge free. In: 48th AIAA/ASME/ASCE/AHS/ASC structures, structural dynamics, and materials conference. American Institute of Aeronautics and Astronautics; 2007.
[16] Evans AG, Hutchinson JW. On the mechanics of delamination and spalling in compressed films. Int J Solids Struct 1984;20(5):455–66.
[17] Yu HH, Hutchinson JW. Influence of substrate compliance on buckling delamination of thin films. Int J Fract 2002;113(1):39–55.
[18] Tarasovs S, Andersons J. Competition between the buckling-driven delamination and wrinkling in compressed thin coatings. Microelectron Reliab 2012;52(1):296–9.